Available online at www.sciencedirect.com
ScienceDirect
Solid State Sciences 9 (2007) 862–868
Solid State Sciences
www.elsevier.com/locate/ssscie

A new polymeric $[Cu(SO_3(CH_2)_3S{-}S(CH_2)_3SO_3)(H_2O)_4]_n$ complex molecule produced from constituents of a super-conformational copper plating bath: Crystal structure, infrared and Raman spectra and thermal behaviour

Miguel A. Pasquale [a], Agustín E. Bolzán [a,*], Jorge A. Güida [b,e,f], Roberto C.V. Piatti [a], Alejandro J. Arvia [a], Oscar E. Piro [c], Eduardo E. Castellano [d]

[a] *Instituto de Investigaciones Fisicoquímicas Teóricas y Aplicadas (INIFTA, CONICET–UNLP), Sucursal 4, Casilla de Correo 16, 1900 La Plata, Argentina*
[b] *CEQUINOR (CONICET-UNLP), Depto. de Quimica, Facultad de Ciencias Exactas, 47 esq. 115, C.C. 962, 1900 La Plata, Argentina*
[c] *Depto. de Física, Facultad de Ciencias Exactas, Universidad Nacional de La Plata and IFLP (CONICET), CC 67, 1900 La Plata, Argentina*
[d] *Instituto de Física de São Carlos, Universidade de São Paulo, CP 369, 13560 São Carlos (SP), Brazil*
[e] *Facultad de Ingeniería (UNLP), 1 esq. 115, 1900 La Plata, Argentina*
[f] *Depto. de Ciencias Básicas, Universidad Nacional de Luján, Luján, Argentina*

Received 28 March 2007; received in revised form 11 May 2007; accepted 12 June 2007
Available online 21 June 2007

Abstract

The formation and characterisation of a polymeric copper complex produced by chemical reaction between copper (II) ions and 3-mercapto-1-propanesulphonate sodium salt (MPSA) were studied. The formation of this complex, followed by sequential UV–visible spectroscopic measurements, involves the reduction of Cu(II) ions to Cu(I) by MPSA, the latter being oxidised to bis-(3-sulphopropyl)-disulphide (SPS), a dimer of MPSA. In the presence of oxygen, the re-oxidation of Cu(I) to Cu(II) results in the formation of polymeric complex species consisting of $[Cu(SO_3(CH_2)_3S{-}S(CH_2)_3SO_3)(H_2O)_4]$ units. Single crystal X-ray diffraction shows that this polymeric copper complex crystallizes in the monoclinic *C*2/*c* space group. The Cu(II) ion in the complex structure lies on an inversion centre in an elongated octahedral environment, equatorially coordinated to four water molecules and axially to two MPSA ligands through one of their sulphonic oxygen atoms. The complex units are arranged in the lattice as polymeric $[Cu(SPS)(H_2O)_4]_n$ molecules extending along the crystal [101] direction. The IR and Raman spectra as well as TGA and DTA data are reported. The stepwise thermal decomposition from room temperature up to 1000 °C begins with the loss of water molecules and ends with the formation of copper sulphide species.
© 2007 Elsevier Masson SAS. All rights reserved.

Keywords: Additives; MPSA; Copper complexes; Electrodeposition; Vibrational spectra; Crystal structure; SPS

1. Introduction

Metal electrodeposit features at solid substrates depend on electrical variables (current, potential and charge passed), substrate nature, cell design, composition of the plating solution and temperature. The presence of adequately chosen additives favours the process in a certain direction and improves the quality of the electrodeposit [1].

Copper deposits on several substrates can be made by either electroless or electroplating utilising different acid and basic copper plating baths [2,3]. These baths consist of a soluble copper salt in low resistivity solutions with a small concentration of additives that are convenient to produce leveling and

* Corresponding author.
E-mail address: aebolzan@inifta.unlp.edu.ar (A.E. Bolzán).

1293-2558/$ - see front matter © 2007 Elsevier Masson SAS. All rights reserved.
doi:10.1016/j.solidstatesciences.2007.06.004

brightening effects at the plated surface. In this respect, in recent years, the super-conformational copper plating became of a particular importance, as it produces a progressive smoothening of the free rough surface consisting of valleys, voids and hills [4,5]. Typical plating baths are aqueous copper sulphate-based solutions containing small amounts of chloride ions, polyethers such as polyethylene glycol (PEG) as a suppressor additive, and a sulphur-containing organic molecule, such as 3-mercapto-1-propanesulphonate sodium salt (MPSA, $Na-SO_3(CH_2)_3SH$) as accelerator and brightener. In this case, one admits that MPSA is largely adsorbed at the valleys and voids allowing the deposition of copper there until they are completely filled, whereas PEG is adsorbed at the top of the hills impeding copper deposition. Experimental data suggest a competitive adsorption between inhibitors and accelerators [6–8] that should depend on the radius of curvature of valleys and hills. At first sight, for these multi-component plating baths there is an important difference between accelerants and suppressors because of the size of their molecules and their difference in the metal–molecule adsorption interactions. This makes the small accelerant molecules to diffuse and migrate inside the voids, whereas the suppressor remains at the top of hills.

On the other hand, sulphur-containing accelerants usually behave as ligands in copper ion-containing aqueous solutions favouring the copper ion complex formation. This is the case of cuprous thiolate that has been identified as the catalyst that accelerates copper deposition [9–12]. The copper electrodeposition rate will depend then on the local cuprous ion concentration at the inner plane of the electrochemical interface [9].

Another common additive used as brightener for copper plating is the MPSA dimer, i.e. the compound 4,5-dithiaoctane-1,8-disulphonic acid (or its disodium salt), also known as bis(sodium-sulphopropyl) disulphide or bis(3-sulphopropyl) disulphide (disodium salt). This compound is best known under the acronym SPS, and will be referred as such in this paper. SPS is a rather unstable compound, the decomposition of which is driven by Cu(I) ions via the formation of a soluble SPS–Cu(I) complex [13]. The latter is produced by the addition of MPSA to aqueous copper sulphate, the yielding of this reaction being highly dependent on whether it takes place in the presence or in the absence of dissolved oxygen [13]. This fact opens the possibility that when Cu(I) ions are present, they could be oxidised to Cu(II) by oxygen yielding hydrogen peroxide and new Cu(II)-complex species.

The above information points out that the chemistry and electrochemistry of constituents of modern copper plating baths are far from being well understood. This work is devoted to the identification of new complex species resulting from the chemical interaction of copper ions and MPSA in aqueous solutions and their participation either directly or indirectly in the super-conformational copper electrodeposition. Accordingly, the formation of a polymeric Cu(II)–SPS complex is reported. Its structure is investigated by X-ray diffraction and characterised by IR and Raman spectroscopies and TGA/DTA analysis. The reported information offers new insights for advancing a more thorough approach to the mechanism of copper electrodeposition from aqueous plating baths containing MPSA and related additives.

2. Experimental

The Cu(II)–SPS complex was prepared by mixing 2 mM MPSA and 1 mM $CuSO_4$ from stock 1 M $CuSO_4$ and 0.5 M MPSA aqueous solution under atmospheric conditions and room temperature. The product was then crystallised by slow solvent evaporation and the crystals were filtered out and dried in a silicagel-containing desiccator.

Under atmospheric conditions, after the addition of the MPSA solution, the initially blue-tinged copper sulphate solution became first yellow, afterwards green and eventually sky blue. This sequential colour change that could be followed throughout the crystallisation stage was not produced under nitrogen saturation. In this case the solution remained yellow and the solvent-free solid residue appeared as a yellow amorphous sticking substance.

The changes in the oxidation state of copper ions in solution during crystallisation were followed by UV–visible spectroscopy utilising an Agilent 8453E UV–visible Spectroscopy System.

The structure of the crystalline sky blue solid product was determined by X-ray diffraction methods using an Enraf–Nonius Kappa CCD diffractometer, working in the ϕ and ω scan mode with Mo Kα, graphite monochromatised, radiation ($\lambda = 0.71073$ Å). Diffraction data were collected with COLLECT [14], reduced with DENZO & SCALEPACK [15] and corrected by absorption effects with PLATON [16] programs. The structure was solved by direct methods employing SHELXS [17] and their non-H atoms refined by anisotropic full-matrix least-squares with the SHELXL [18] program. The ligand CH_2 hydrogen atoms were included in the molecular model at stereo chemical positions and refined with the riding model. The water H-atoms were located in a difference Fourier map and refined isotropically with O–H distances restrained to a target value of 0.88(1) Å. Crystal data and refinement results are summarized in Table 1.

The infrared spectra (KBr pellets) were recorded with an FTIR Bruker 113v spectrophotometer equipped with a mid IR DTGS detector. Raman spectra were obtained at room temperature with an FTIR Bruker 66 spectrophotometer fitted with the NIRR attachment. These measurements were obtained for 2 and 4 cm^{-1} resolutions, utilising a rotary cell to avoid the decomposition of sample due to the intensity of the laser beam (Nd-YAG).

Thermo-gravimetric (TGA) and differential thermal analyses (DTA) were performed on a Shimadzu system (models TG-50 and DTA-50, respectively), working under nitrogen at 50 ml min^{-1} flow rate and 10 °C min^{-1} heating rate, and samples' weights ranged between 9 and 15 mg. Al_2O_3 was used as DTA standard.

Residues obtained in TGA measurements were analysed by powder X-ray diffractometry. For this purpose a PANalytical XPert PRO diffractometer using CuKα radiation

Table 1
Crystal data and structure refinement results

Empirical formula	$C_6H_{20}CuO_{10}S_4$
Formula weight	444.00
Crystal system	Monoclinic
Space group	*C*2/*c* (No. 15)
a (Å)	24.547(1)
b (Å)	9.7033(4)
c (Å)	7.2799(4)
β (°)	104.354(3)
V (Å^3)	1679.9(1)
Z	4
ρ (calc) (Mg/m^3)	1.756
μ(Mo Kα) (mm^{-1})	1.837
F(000)	916
Crystal size (mm)	0.18 × 0.08 × 0.02
Crystal color/shape	Pale blue/prism
θ Range for collection (°)	2.27–25.00
Index ranges	$-29 \le h \le 29$, $-11 \le k \le 11$, $-8 \le l \le 8$
Reflections collected/unique	9194/1491 [*R*(int) = 0.0718]
Observed reflections [$I > 2\sigma(I)$]	1022
Completeness (%)	99.9 (to $\theta = 25.00$)
Weights, *w*	$[\sigma^2(F_0^2) + (0.0798P)^2 + 9.71P]^{-1}$
	$P = [\mathrm{Max}(F_0^2,0) + 2F_c^2]/3$
Data/restraints/parameters	1491/4/113
Goodness of fit on F^2	1.032
Final *R*-index[a] [$I > 2\sigma(I)$]	$R1 = 0.0523$, $wR2 = 0.1371$
R indices (all data)	$R1 = 0.0814$, $wR2 = 0.1576$
Largest peak and hole (e.A^{-3})	0.796 and −0.790

[a] $R_1 = \sum ||F_o| - |F_c|| / \sum |F_o|$; $wR_2 = [\sum w(F_o^2 - F_c^2)^2 / \sum w(F_o^2)^2]^{1/2}$.

($\lambda = 1.540$ Å) at 40 kV and 40 mA was employed. The patterns were recorded for $5° \le 2\theta \le 70°$ with a scan step time of 1 s and a step size of 0.02°.

3. Results and discussion

3.1. The process of the $[Cu(SO_3(CH_2)_3S{-}S(CH_2)_3SO_3)(H_2O)_4]_n$ formation

During the formation and crystallisation of the Cu–SPS complex in the aqueous environment the first colour change, from blue to yellow and to sky blue, suggests the likely transformation of Cu(II) ions to Cu(I) and vice-versa. These changes in the oxidation state of copper ions were followed by UV–visible spectroscopy between 200 and 900 nm for both MPSA-free and 0.5 M MPSA-containing 1 M $CuSO_4$ aqueous solutions (Fig. 1). In the absence of MPSA there is an absorption band with a maximum at 790 nm due to the electronic transitions of aqueous Cu(II) ions, whereas immediately after the addition of aqueous MPSA to the $CuSO_4$ solution the above absorption band at 790 nm disappears. This fact points out a chemical reduction of Cu(II) ions by MPSA yielding aqueous Cu(I) ions. For the latter, the electronic transitions at 790 nm is absent because of their d^{10} electronic configuration. Therefore, the redox process can be expressed as

$$2Cu^{2+} + 2e^- = 2Cu^+ \quad (1)$$

accompanied by the oxidation of the thiol group of MPSA yielding a dimer in which an S–S bond is involved

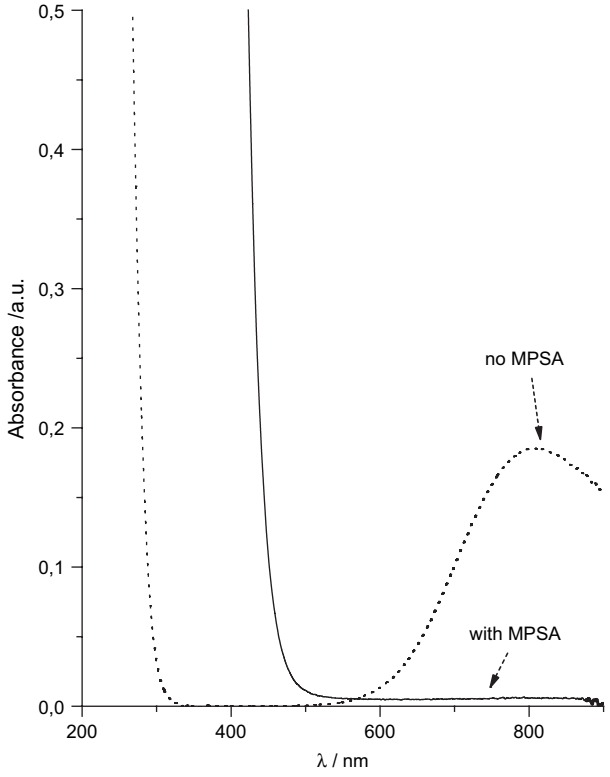

Fig. 1. UV–visible absorbance spectra of aqueous 0.5 M $CuSO_4$ in the absence of MPSA and after the addition of aqueous 1 M MPSA at 298 K.

$$2\left[HS(CH_2)_3SO_3\right]^- = \left[S(CH_2)_3SO_3\right]_2^{2-} + 2H^+ + 2e^- \quad (2)$$

The dimer formation is supported by XRD data, as shown further on. Redox reactions such as (1) and (2) are known to occur with thioureas in the presence of Cu(II) ions [19].

It should be noted that the reduction product in Eq. (2), i.e. 4,5-dithiaoctane-1,8-disulphonic acid or sulphopropyl sulphonate (SPS), is a well-known additive for metal plating baths, although it is rather unstable under open circuit conditions [20]. In this case the formation of the Cu(I)–SPS complex in solution in the absence of dissolved oxygen has been suggested from HPLC, UV–visible and SECM measurements [13]. The Cu(I)–SPS complex imparts a yellowish tinge to the solution.

Crystallisation of Cu(I)–SPS under atmospheric conditions favours the change in the colour of the solution backwards to sky blue suggesting the reappearance of Cu(II) ions. Therefore, firstly formed Cu(I) ions by reactions (1) and (2) are re-oxidised to Cu(II) by oxygen in solution according to the following redox reactions

$$2Cu^+ = 2Cu^{2+} + 2e^- \quad (3)$$

$$\frac{1}{2}O_2 + 2H^+ + 2e^- = H_2O \quad (4)$$

the protons for reaction (4) being provided by reaction (2). In this case, the sequential UV–visible spectra recorded during crystallisation show that the intensity of the 790 nm band steadily increases (Fig. 2). As the SPS molecule is involved

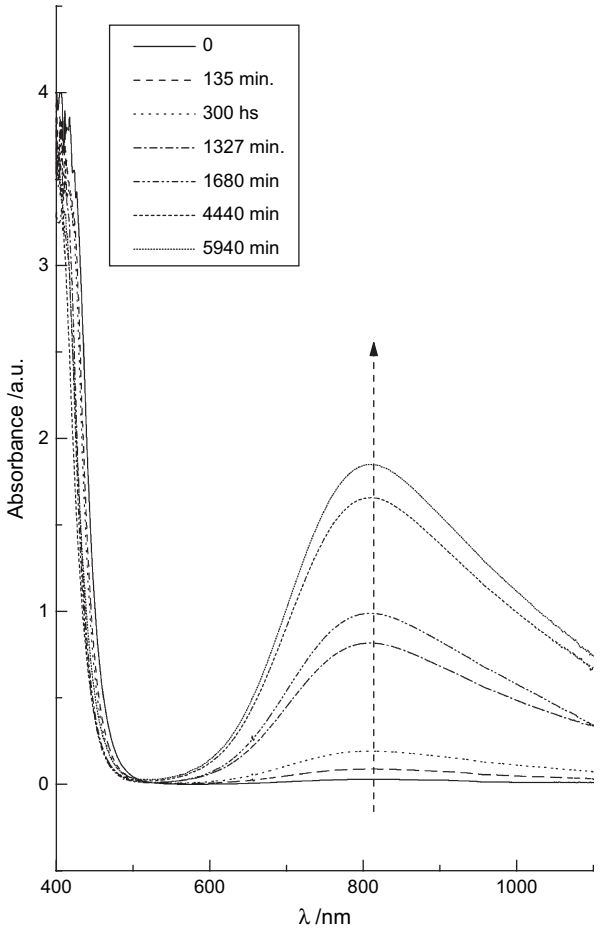

Fig. 2. Time dependence of the UV–visible spectrum of 0.5 M MPSA + 1 M $CuSO_4$ aqueous solutions at 298 K.

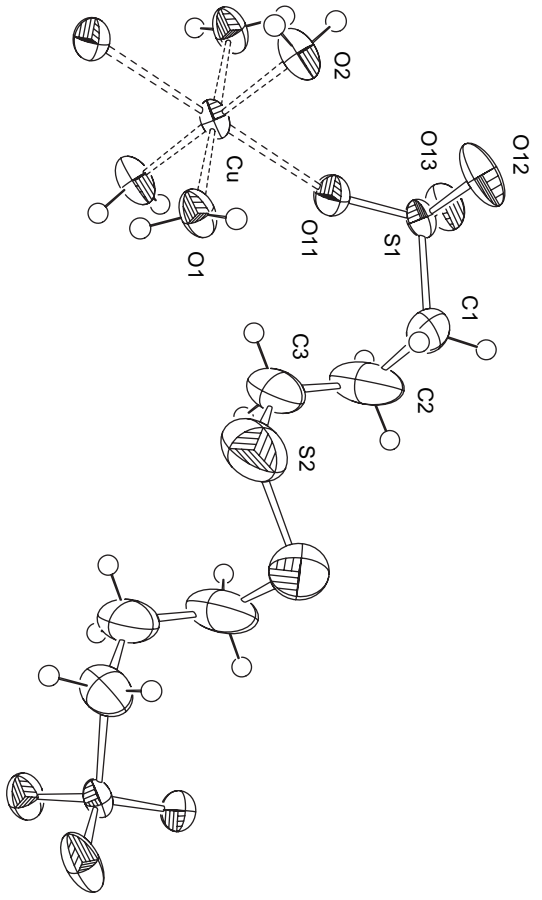

Fig. 3. Molecular plot of the $[Cu(SPS)(H_2O)_4]$ complex molecule showing the labeling of the independent non-H atoms and their displacement ellipsoids at the 50% probability level. The copper(II) ion is sited at a crystallographic inversion centre and the unlabelled half of the SPS ligand is related to the labeled one by a two-fold axis through the mid point of the disulphide S–S bond. Copper–ligand bonds are indicated by dashed lines.

in the Cu–SPS complex structure, as concluded from XRD data (see below), its contribution to the redox process (3)–(4) can be disregarded. Then, the main product resulting from the reaction between aqueous Cu(II)- and MPSA-containing solution is a polymer consisting of single Cu(II) ion and SPS ligand units. This conclusion is also supported by XRD and FTIR data.

3.2. The crystal structure of polymeric $[Cu(SO_3(CH_2)_3S–S(CH_2)_3SO_3)(H_2O)_4]_n$

An ORTEP [21] drawing of the molecule is shown in Fig. 3. Selected intra-molecular bond distances and angles are reported in Table 2.

The crystal structure shows that the Cu(II) ion is sited on a crystallographic inversion centre in an elongated octahedral environment, equatorially coordinated to four water molecules [Cu–Ow bond distances of 1.956(4) and 1.960(4) Å] and axially to two sulphonic oxygen atoms [d(Cu–O) = 2.344(4) Å] belonging to inversion related SPS ligands. The ligand $SO_3(CH_2)_3S–S(CH_2)_3SO_3$ molecule, in turn, is sited on a crystal two-fold axis passing through the mid point of the disulphide S–S bond. The diagonal glide plane containing the copper ion generates a polymeric $[Cu(SPS)(H_2O)_4]_n$ structure extending along the lattice [101] direction containing alternated crystallographic inversion centres (copper sites) and two-fold axes (SPS sites). This is shown in the PLUTON [14] plot of Fig. 4.

Table 2
Selected bond distances (Å) and angles (°) in $[Cu(SPS)(H_2O)_4]_n$

Bond distances	
Cu–O(1)	1.956(4)
Cu–O(2)	1.960(4)
Cu–O(11)	2.344(4)
S(2)–S(2″)	2.011(6)
Bond angles	
O(1)–Cu–O(2)	89.7(2)
O(1′)–Cu–O(2)	90.3(2)
O(1)–Cu–O(11′)	88.9(2)
O(1)–Cu–O(11)	91.1(2)
O(2)–Cu–O(11)	89.5(2)
O(2)–Cu–O(11′)	90.5(2)
C(3)–S(2)–S(2″)	104.4(4)

Primed atoms are symmetry related to unprimed ones through the inversion operation $-x+3/2,-y+1/2,-z+1$. S(2″) atom is symmetry related to S(2) by the two-fold rotation $-x+2,y,-z+3/2$.

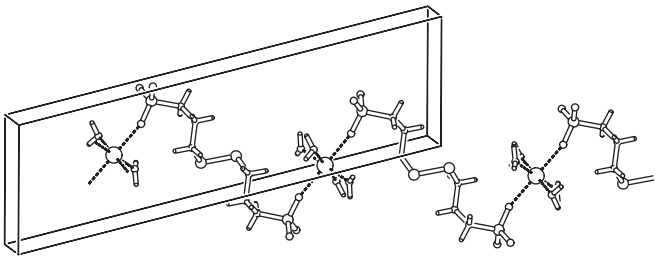

Fig. 4. Projection down the crystal unique *b*-axis showing the polymeric structure of $[Cu(SPS)(H_2O)_4]_n$ as it extends along the [101] direction. The crystal *c*-axis is along the vertical. Neighboring $[Cu(SPS)(H_2O)_4]$ monomers on the polymer are symmetry related to each other through the diagonal glide plane containing the copper ion.

The crystal is further stabilized by inter-polymer Ow–H···O bonds, involving as donors the two independent water molecules on a given chain and as H-bond acceptors the two un-bonded-to-metal oxygen sulphonic atoms of neighboring polymers. H-bond distances and angles are detailed in Table 3. There it can be appreciated that the w1 water molecule is the most tightly held as it forms a relatively strong and linear H-bond [Ow1···O distance of 2.715 Å and Ow1–H···O angle of 174.7°].

4. Vibrational spectra

The assignments of the vibrational spectra of the polymeric complex (Table 4) were carried out taking into account both data previously reported [22–24] and the comparison to the spectra of MPSA.

In the region of high wavenumbers two sharp bands are observed at 3597 and 3528 cm^{-1}. These bands are superimposed onto a broad band centred at ca. 3370 cm^{-1}. All these features are assigned to the O–H stretching vibration of two different water molecules in the lattice. These water molecules are H-bonded to neighboring sulphonic oxygen atoms (see Table 3). The sharp O–H bands can be assigned to the w2 water molecules while the broad one can be attributed to the more strongly H-bonded w1 water molecule.

At 2970 and 2923 cm^{-1} the weak bands related to the asymmetric and symmetric stretching modes of C–H groups appear, respectively, with a blue-shift of ca. 20 cm^{-1} with respect to the position of the band in the MPSA. In the Raman spectrum a strong absorption band at 2923 cm^{-1} is due to the symmetric stretching of the C–H bond.

Table 3
Hydrogen bonds in $[Cu(SPS)(H_2O)_4]_n$

D–H	*d*(D–H)	*d*(H···A)	∠D–H···A	*d*(D···A)	A	Symmetry operation
O1–H11	0.874	1.887	161.57	2.730	O12	$[x,y,z+1]$
O1–H12	0.874	1.843	174.69	2.715	O12	$[x,-y+1,z+1/2]$
O2–H21	0.877	1.936	165.43	2.794	O13	$[-x+3/2,y+1/2,-z+1/2]$
O2–H22	0.877	1.886	163.00	2.738	O13	$[-x+3/2,-y+1/2,-z]$

Table 4
Principle IR and Raman bands (in cm^{-1}) of $[Cu(SPS)(H_2O)_4]_n$

IR	Raman	Assignment
3597		ν_a H_2O
3528		ν_s H_2O
2970		ν_a C–H
2923	2923	ν_s C–H
		ν S–H
1627		δ H_2O
1445		δ CH_2–S
1415		δ CH_2
1251		ω CH_2
1203		ν_a SO_3^{2-}
	1065	ν_s SO_3^{2-}
1050	1055	ν_s SO_3^{2-}
739	739	ρ CH_2 (ν C–S)
733		ρ CH_2
638	638	ν C–S
532		δ SO_3
	506	ν S–S

While the Raman spectrum of MPSA shows a very strong band at 2552 cm^{-1} related to the S–H stretching, this band is no longer observed in the spectra of the polymeric copper complex due to the formation of the S–S bridge. The S–S stretching band is too weak to be observed in the IR spectrum, but appears as a medium band at 506 cm^{-1} in the Raman spectrum. It should be noted that the relative intensity of IR and Raman bands depends firmly on the orientation of groups bonded at both sides of the S–S bridge. In the polymer both sides around the S–S bridge are symmetric, therefore, the Raman intensity of the S–S stretching mode is expected to be stronger than that of the infrared one (Fig. 5).

In the region 2000–1000 cm^{-1}, the bending mode of the water molecules is observed at 1627 cm^{-1}. This band appears rather asymmetric suggesting that it comprises two bands related to water molecules in a different environment, as described above. The bands at 1445 and 1415 cm^{-1} are assigned to the deformation mode of the CH_2 group.

In the very complex region between 1300 and 1000 cm^{-1} absorption bands due to both sulphonic and methylene groups

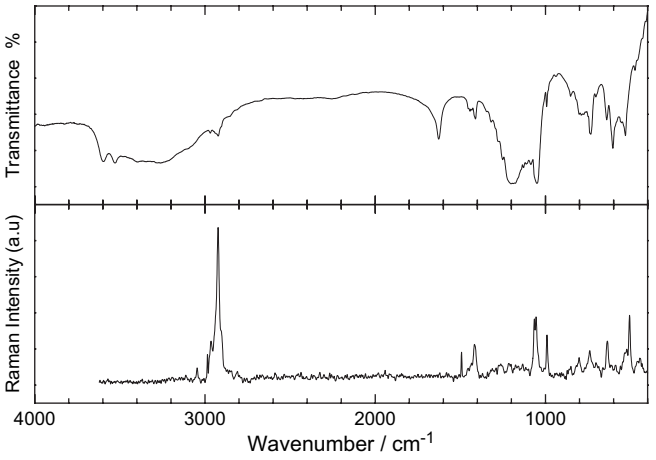

Fig. 5. IR and Raman spectra of $[Cu(SPS)(H_2O)_4]_n$ at 298 K.

are expected. The strong bands at 1203 and 1050 cm^{-1} are assigned to the asymmetric and symmetric stretching modes of $-SO_3$, respectively. The symmetric stretching modes give rise to strong bands in the Raman spectrum at 1065 and 1055 cm^{-1}.

The region between 1000 and 400 cm^{-1} shows the rocking mode of CH_2 at 739 cm^{-1} and the C–S stretching mode at 638 cm^{-1}. Eventually, the bending mode of the SO_3 group appears at 532 cm^{-1}.

5. Thermal behaviour of the $[Cu(SO_3(CH_2)_3S-S(CH_2)_3SO_3)(H_2O)_4]_n$ complex

The thermal behaviour of the copper–SPS complex polymer was investigated by TGA and DTA under nitrogen from room temperature up to 1000 °C. These measurements were complemented by IR spectra of residues obtained at 175, 270, 450 and 1000 °C.

Both the TGA and the DTA curves (Fig. 6) show that the degradation process of the molecule is very complex and consequently no simple degradation pathway can easily be established. The TGA curve exhibits a series of steps related to the thermal degradation of the polymer. This process involves several consecutive stages with a pronounced difference in their mass loss. The greatest mass loss is observed between 200 and 250 °C, and 300 and 450 °C. According to the DTA curve the thermal decomposition of the copper complex consists of a number of sequential endothermic processes.

Despite those drawbacks, the TGA and DTA data show that first water molecules are released entirely in the temperature range from 25 to 160 °C. This process occurs in three steps, the first one involves a mass loss of 8.04%, in excellent agreement with the value calculated for the loss of two water molecules per chemical formula (8.11%), as the IR spectrum of the residue obtained at 175 °C showed the absence of absorption bands at 3528 and 3597 cm^{-1} related to w2. The second and third ill-defined steps related to the loss of water are recorded at ca. 116 and 180 °C, both processes are characterised by endothermic peaks in the DTA (Fig. 6).

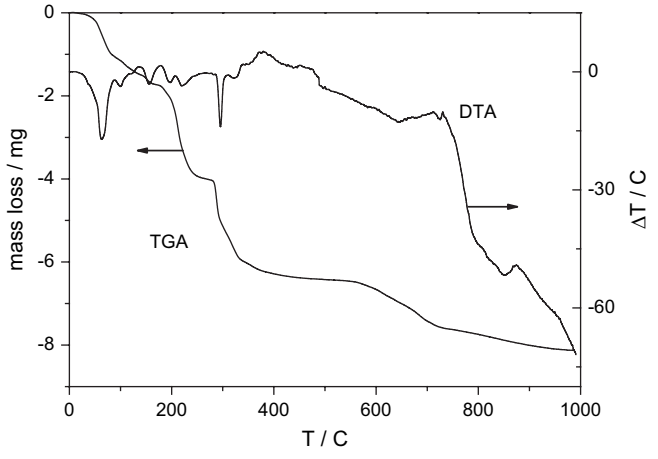

Fig. 6. Thermo-gravimetric and DTA curves for the thermal decomposition of $[Cu(SPS)(H_2O)_4]_n$ run under nitrogen. Weight of the sample: 12.8 mg, heating rate: 10 °C min^{-1} at 298 K.

Between 270 and 450 °C the IR spectrum of the residue at 450 °C indicates no absorption bands related to sulphonate groups. The loss of two sulphonate groups involves 21.6% of the total polymer mass, a figure that agrees reasonably well with the experimental value $20 \pm 1\%$. Furthermore, the global mass loss at 450 °C results in $50 \pm 2\%$, a value consistent with the loss of both water molecules and sulphonate groups. In fact, the solid spongy-like black residue produced between 320 and 450 °C exhibits a significant increase in apparent volume as compared to the solid residue obtained at lower or higher temperatures. This is due to the formation of either gaseous SO_2 or SO_3 during the thermal decomposition of the product up to 450 °C.

Powder X-ray diffraction data of the residue obtained at 450 °C exhibit mainly peaks related to the presence of cupric sulphide species, although the presence of some non-stoichiometric copper sulphides cannot be disregarded.

The final black residue resulting at 1000 °C consists of about 36% of the initial polymer mass, a figure that coincides with the formation of Cu_2S. The IR spectrum of this residue shows two major bands at 1118 and 617 cm^{-1} that also agree with the formation of Cu_2S.

6. Conclusions

The formation of a polymeric complex species produced from the interaction of MPSA with Cu(II) ions in aqueous solutions was established. UV–visible spectroscopic experiments indicate that the formation of this polymeric complex begins with the initial reduction of Cu(II) to Cu(I) ions and the simultaneous oxidation of MPSA to SPS species through the formation of an S–S bridge. Under atmospheric conditions the aqueous Cu(I) ions are oxidised to Cu(II) by the presence of oxygen in the solution producing the polymeric structure $[Cu(SO_3(CH_2)_3S-S(CH_2)_3SO_3)(H_2O)_4]_n$. The crystal structure of this polymeric complex, resolved by X-ray diffraction methods, shows a Cu(II) ion lying on an inversion centre in an elongated octahedral environment, equatorially coordinated to four water molecules and axially to two MPSA ligands through one of their sulphonic oxygen atoms. This polymeric complex was characterised by IR and Raman spectroscopies. The thermal behaviour, studied by TGA and DTA, shows that the decomposition of the polymeric complex takes place in several steps starting with the release of the water molecules and ending with the formation of copper sulphide species. The discovery of this polymeric complex, produced from constituents of super-conformational copper plating baths that contain MPSA and related additives, provides new insights for advancing in the study of the mechanism of copper electrodeposition.

Supplementary material: crystallographic data (excluding structure factors) have been deposited with the Cambridge Crystallographic Data Centre, CCDC No. 620821. Copies of this information may be obtained free of charge from the director, CCDC, 12 Union Road, Cambridge CB2 1EZ, UK.

Acknowledgements

This work was supported by ANPCYT (PICT 12508/02), CONICET (Argentina) and FAPESP (Brazil). Some of the X-ray diffraction experiments were carried out at the National Diffraction Laboratory (LANADI), La Plata, Argentina. A.E.B. is member of the Research Career of CICPBA (Argentina). M.A.P., A.J.A. and O.E.P. are research fellows of CONICET.

Appendix. Supplementary data

Supplementary data associated with this article can be found, in the online version, at doi:10.1016/j.solidstatesciences.2007.06.004.

References

[1] M. Schlesinger, M. Paunovic, Modern Electroplating, 4th ed. Wiley, New York, 2000.
[2] R. Sard, J. Electrochem. Soc. 117 (1970) 864.
[3] P.C. Andricacos, C. Uzoh, J.O. Dukovic, J. Horkans, H. Deligianni, IBM J. Res. Dev. 42 (1998) 567.
[4] T.P. Moffat, D. Wheeler, W.H. Huber, D. Josell, Electrochem. Solid State Lett. 148 (2001) C26.
[5] A.C. West, S. Mayer, J. Reid, Electrochem. Solid State Lett. 4 (2001) C50.
[6] V.D. Jovic, B.M. Jovic, J. Serb. Chem. Soc. 66 (2001) 935.
[7] T.P. Moffat, J.E. Bonevich, W.H. Huber, A. Stanishevsky, D.R. Kelly, G.R. Stafford, D. Josell, J. Electrochem. Soc. 147 (2000) 4524.
[8] M.A. Pasquale, D.P. Barkey, A.J. Arvia, J. Electrochem. Soc. 152 (2005) C149.
[9] P.M. Vereecken, R.A. Binstead, H. Delegianni, P.C. Andricacos, IBM J. Res. Dev. 49 (2005) 1.
[10] J.P. Healy, D. Pletcher, M. Goodenough, J. Electroanal. Chem. 338 (1992) 167.
[11] J.P. Healy, D. Pletcher, M. Goodenough, J. Electroanal. Chem. 338 (1992) 179.
[12] J.J. Kim, S.-K. Kim, Y.S. Kim, J. Electroanal. Chem. 542 (2003) 61.
[13] A. Frank, A.J. Bard, J. Electrochem. Soc. 150 (2003) C244.
[14] Enraf-Nonius. COLLECT, Nonius BV, Delft, The Netherlands, 1997–2000.
[15] Z. Otwinowski, W. Minor, in: J.C.W. Carter, R. Sweet (Eds.), Methods in enzymology, Academic Press, New York, 1997, pp. 307–326.
[16] A.L. Spek, PLATON: A Multipurpose Crystallographic Tool, Utrecht University, Utrecht, The Netherlands, 1998.
[17] G.M. Sheldrick, SHELXS-97: Program for Crystal Structure Resolution, University of Göttingen, Göttingen, Germany, 1997.
[18] G.M. Sheldrick, SHELXL-97: Program for Crystal Structures Analysis, University of Göttingen, Göttingen, Germany, 1997.
[19] A.E. Bolzán, I.B. Wakenge, R.C.V. Piatti, R.C. Salvarezza, A.J. Arvia, J. Electroanal. Chem. 501 (2001) 241.
[20] J.P. Healy, D. Pletcher, M. Goodenough, J. Electroanal. Chem. 338 (1992) 155.
[21] C.K. Johnson, ORTEP-II. A Fortran Thermal-Ellipsoid Plot Program. Report ORNL-5318, Oak Ridge National Laboratory, Tennessee, USA, 1976.
[22] N.B. Colthup, L.H. Daly, S.E. Wiberley, Introduction to Infrared and Raman Spectroscopy, 3rd ed. Academic Press, New York, 1990.
[23] H. Günzler, H.-U. Gremlich, IR Spectroscopy, Wiley-VCH Verlag GmbH, Weinheim, 2002.
[24] M.G. Miles, G. Doyle, R.P. Cooney, R.S. Tobias, Spectrochim. Acta, Part A: Mol. Spectrosc. 25 (1969) 1515.